

Renormalization group study of the soliton mass in the (1 + 1)-dimensional $\lambda\Phi^4$ lattice model

J. C. Ciria and A. Tarancón

Departamento de Física Teórica, Facultad de Ciencias, Universidad de Zaragoza, C/Pedro Cerbuna 12, 50009 Zaragoza, Spain

(Received 22 March 1993)

We compute, in the (1 + 1)-dimensional ($\lambda\Phi^4$) model on the lattice, the soliton mass by means of two very different numerical methods. First, we make use of a “creation operator” formalism, measuring the decay of a certain correlation function. Second, we measure the shift of the vacuum energy between the symmetric and the antiperiodic systems. The obtained results are fully compatible. We compute the continuum limit of the mass from the perturbative renormalization group equations. Special attention is paid to ensure that we are working in the scaling region, where physical quantities remain unchanged along any renormalization group trajectory. We compare the continuum value of the soliton mass with its perturbative value up to one-loop calculation. Both quantities show a quite satisfactory agreement. The first is slightly bigger than the perturbative one; this may be due to the contributions of higher-order corrections.

PACS number(s): 05.50.+q, 11.10.Gh

I. INTRODUCTION

Standard perturbation is known to be a useful tool for the formulation of quantum field theory starting from classical field theory. It has, however, serious handicaps such as the fact that nonperturbative effects are not taken into account. An alternative possibility is the quantization of nontrivial, nonperturbative solutions to the classical equations, such as solitons.

The study of such topologically nontrivial vacua in field theories presents several problems when the model is formulated in the continuum or on the lattice. In the continuum it is very difficult to extract nonperturbative quantities, such as mass, and on the lattice, where this is possible with Monte Carlo simulations, other problems are present.

First, on the lattice the analysis of this kind of configuration is made difficult by the trivial topology of the lattice, and because the concept of continuity is lost [1]. Second, it is of fundamental importance to define how to measure quantities on these topologically nontrivial vacua [2]. We can consider how to compute the mass, for instance. As is known, solitons are characterized by a topological charge, related to their behavior when spatial coordinates tend to infinity [$Q \sim \Phi(x \rightarrow \infty) - \Phi(x \rightarrow -\infty)$]. This charge is conserved with time. When we quantize a soliton, we obtain a quantum soliton particle and a series of excitations of this particle, a so-called soliton sector. Topological charge becomes then a quantum number characterizing the sector. Its conservation prevents the soliton from falling to the vacuum, ensuring its stability. The standard way of calculating the mass is considering an operator with nonvanishing projection on this sector, then computing the connected correlation to large distance, and finally extracting the mass from the coefficient of the exponential decay.

In the general case, for topologically nontrivial sectors, the definition of such an operator is very ambiguous. It is

possible to define many operators on the lattice sharing the same continuum limit, although their behavior far from this limit differs from each other. On the lattice, the region where we can obtain results within reasonable computation times is generally far from the continuum limit, where very big sizes would be necessary, and all those continuum-equivalent operators give us different results [3].

In four-dimensional theories computer limitations have made this point particularly difficult. Fortunately, some interesting facts can be studied quite satisfactorily in less than four dimensions. We consider on this paper the (1 + 1)-dimensional $\lambda\Phi^4$ [$(\lambda\phi^4)_{1+1}$] model, where solitons are also present.

On a finite lattice the boundary conditions fix up the topological sector. Periodic conditions fix the trivial vacua, for instance. Antiperiodic conditions fix vacua with nontrivial topology (if the symmetry is broken). Only free boundary conditions allow us to have different topological sectors; however the finiteness of the system allows us to travel between vacua, and we finish always in the trivial sector, the energy of which is lower.

In this model it is possible to carry out the computation of the soliton mass by using two different, related, methods.

First, we have made use of the operator defined by Kadanoff and Ceva [5]; in spin systems, its effect can be seen as the introduction of a twist: a topological excitations induced by a specific dislocation of the lattice. It has a topological charge different from zero. Consequently, we expect a nonzero projection onto the soliton sector.

On the other hand, we can consider the system with antiperiodic spatial conditions for the scalar field. This system can be considered as the periodic one after the introduction of a twist along the whole lattice time. The difference of the energies of the periodic and antiperiodic systems, which is a local, easy to measure quantity, provides us with another method to compute the soliton mass.

We always keep in mind that a theory in a lattice acquires physical meaning only when we make its spacing tend to zero. In order to get to the continuum limit [4] we use the renormalization group (RG) equations, which are known in this model. We must consider the limit of zero lattice spacing. A change in this spacing, and a change in the coupling constants in such a way that the physical observables remain unchanged, can be carried out by using the RG equations.

Iterating RG transformations, we obtain a series of points in the parameter space, a renormalization group trajectory (RGT), which can be characterized by a parameter l . Different points of a trajectory, corresponding to different values of the parameters, are obtained after integrating over successive energy scales. Thus, when we move on any RGT, the physics remains the same. In this way, for example, as we evolve on a RGT, we see different values of the correlation length on lattice units, $\xi_0(l)$, but this correlation in physical units $\xi = a(l)\xi_0(l)$ remains constant.

A. $\lambda\phi^4$ model

We study the $\lambda\phi^4$ model in $d=2$ dimensions, the Euclidean Lagrangian density of which is given by

$$S_{\text{Euc}} = \frac{1}{2} \int_p (p^2 + r_0) \Phi(p) \Phi(-p) + \frac{\lambda_0}{4!} \int_{p_1} \int_{p_2} \int_{p_3} \Phi(p_1) \Phi(p_2) \Phi(p_3) \Phi(-p_1 - p_2 - p_3), \quad (4)$$

with $\int_p \equiv \int_0^1 d^d p / (2\pi)^d$. In $d=2$ we have two fixed points [4].

(i) The Gaussian point, $S_{\text{Gauss}} = \int_p u_2^*(p) \Phi(p) \Phi(-p)$, with $u_2^*(p) \sim p^2$, that is to say, taking just the kinetic part of the Lagrangian.

(ii) A nontrivial point, which is built adding to the Lagrangian the term

$$S = \int_{q_1} \int_{q_2} \int_{q_3} u_4^*(q_1, q_2, q_3, -q_1 - q_2 - q_3) \Phi(q_1) \Phi(q_2) \Phi(q_3) \Phi(-q_1 - q_2 - q_3), \quad (5)$$

with $u_4^*(q_1 \cdots q_4) \sim (q_1^2 + \cdots + q_4^2)$.

The $\lambda\Phi^4$ model in less than four dimensions is superrenormalizable. The only divergent graph is that of one vertex with two external legs and a loop. We can get rid of this divergence simply by renormalizing the mass, and therefore it is not necessary to renormalize λ ; we can keep it fixed all the time as we make a go to 0 (equivalently, $\Lambda \rightarrow \infty$). Since $\lambda = \lambda_0 a^{-2}$, it implies $\lambda_0 \rightarrow 0$ as a^2 . In our lattice, consequently, in the continuum limit $u_4^* = \lambda_0^* = 0$, we are considering the Gaussian fixed point. Our RGT will evolve in its attraction domain.

We follow the renormalization group scheme; in order to permit a continuous evolution in the parameter space, we allow integrations of the variable p between $1/s$ and 1 . Linearizing the resulting equations near the critical point, we obtain [7]

$$\hat{\lambda}_0 = s^{4-d} \lambda_0, \quad \hat{r}_0 = s^2 \left[r_0 + \frac{\lambda_0}{4\pi} \ln s \right], \quad (6)$$

where $\hat{\lambda}_0$ and \hat{r}_0 are the transforms of λ_0 and r_0 .

These expressions have a limited region of validity: for big values of λ_0, r_0 , the linear approximation is not valid.

$$\mathcal{L}_{\text{Euc}} = \frac{1}{2} (\partial_\mu \Phi)^2 + \frac{r}{2} \Phi^2 + \frac{\lambda}{4!} \Phi^4, \quad (1)$$

where Φ is dimensionless, $[\lambda] = l^{-2}$, $[r] = l^{-2}$.

In order to adapt our Lagrangian to the lattice, we proceed as usual:

$$\int_0^L dx \rightarrow a^d \sum_{n=0}^{L/a}, \quad \partial_\mu \Phi \rightarrow \frac{\Phi[(n+\mu)a] - \Phi[na]}{a}, \quad (2)$$

where L is the lattice extension. We conclude

$$S_{\text{Euc}} = - \sum_{n,\mu} \Phi_n \Phi_{n,\mu} + \sum_n \left[\left(d + \frac{r_0}{2} \right) \Phi_n^2 + \frac{\lambda_0}{4!} \Phi_n^4 \right]. \quad (3)$$

We introduce the following notation: the dimensionless parameters defined on the lattice are subscripted; thus we use λ_0, r_0 (respectively equal to $\lambda a^2, r a^2$).

Making the spatial coordinates discrete implies imposing a momentum cutoff $\Lambda = 2\pi/a$. After scaling the momenta $q \rightarrow p = q/\Lambda$ we can express (3) in momentum space [4]:

On the other hand, for small values of the parameters, we are very near the Gaussian point, the correlation length becomes very large, and if it is of the order of the lattice size, finite-size effects mask our results. We refer to the intermediate region where the continuum is reproduced as the scaling region.

We remark that the fact of staying in the basin of attraction of a Gaussian fixed point does not prevent at all the possibility of spontaneous symmetry breaking. Given one point (λ_0, r_0) in the parameter space, the renormalization group trajectory starting from it cannot cross the transition line between the $\langle \Phi^2 \rangle = 0$ and $\langle \Phi^2 \rangle \neq 0$ phases; it remains in the phase to which the initial point belongs. Thus, if we start in the symmetry broken phase, the continuum limit of our theory presents symmetry breaking.

II. COMPUTATION OF THE SOLITON AND FUNDAMENTAL BOSON MASSES

A. Fundamental boson

In order to calculate the mass of the fundamental boson m_ρ we use the connected correlation function be-

tween the Higgs fields, $\langle \Phi(\mathbf{x},0)\Phi(\mathbf{x},t) \rangle$. In order to avoid contributions from states with nonzero momenta, we integrate on \mathbf{x} and consider [6]

$$C_\phi(t) = \langle \phi(t)\phi(0) \rangle, \quad (7)$$

where $\phi(t) = \int d\mathbf{x} \phi(\mathbf{x},t)$. For large t , and if the correlation length is different from zero, $C_\phi(t)$ behaves, on an infinite lattice, as $C_\phi(t) \sim \exp(-mt)$.

We consider periodic boundary conditions in our lattice, L being its extent. Consequently, the point n is equivalent to $n+L$. Given two points at a distance t , there are two possible paths connecting them: one of length t and the other, resulting from the boundary conditions, the length of which is $L-t$. Thus, the mass is given by

$$\langle \phi(t)\phi(0) \rangle \simeq e^{-mt} + e^{-m(L-t)} \quad (8)$$

so that

$$\frac{C_\phi(n+1)}{C_\phi(n)} = \frac{\cosh[m_\rho(n+1-L/2)]}{\cosh[m_\rho(n-L/2)]}, \quad (9)$$

where a is the time spacing of the lattice. We can solve (9) and obtain a series of values of $m_\rho(n)$ depending on n . For small n they have contributions from large mass states, and for large n the signal is small; there is an intermediate region of n where $m_\rho(n)$ is nearly constant. We take it as the actual value of the mass.

B. Soliton mass

Kadanoff [5] introduces the correlation function between two points in the dual space R_1, R_2 , $\langle \mu_{R_1}\mu_{R_2} \rangle$ in the following way: we start from a Lagrangian $S = \sum_{n,\mu} J_{n,\mu} \Phi_n \Phi_{n+\mu} + \sum_n \mathcal{O}(\Phi_n)$; we draw a path in the dual space connecting the dual points R_1 and R_2 , and change the sign of the coupling constants J 's placed on the links crossed by our path. We have

$$\langle \mu_{R_1}\mu_{R_2} \rangle = \frac{1}{Z} \sum_{[\phi]} \exp \left[- \sum_{n,\mu}^* J_{n,\mu} \Phi_n \Phi_{n,\mu} + \sum'_{n,\mu} J_{n,\mu} \Phi_n \Phi_{n,\mu} \right], \quad (10)$$

where $\sum_{[\phi]}$ runs over all the configurations of the field, $\sum_{n,\mu}^*$ takes into account the links with their signs changed and $\sum'_{n,\mu}$ refers to the rest of the links. Equivalently,

$$\langle \mu_{R_1}\mu_{R_2} \rangle = \frac{1}{Z} \sum_{[\Phi]} \exp \left[S - 2 \sum_{n,\mu}^* J_{n,\mu} \Phi_n \Phi_{n,\mu} \right] = \left\langle \exp \left[-2 \sum_{n,\mu}^* J_{n,\mu} \Phi_n \Phi_{n,\mu} \right] \right\rangle, \quad (11)$$

where S is the original action.

We can alternatively express the correlation function in terms of a "twisted action" $S_t = S - 2 \sum_{n,\mu}^* J_{n,\mu} \Phi_n \Phi_{n,\mu}$, with its corresponding partition function $Z_t = \sum_{[\Phi]} \exp\{-S_t\}$, that is to say,

$$\langle \mu_{R_1}\mu_{R_2} \rangle = \frac{Z_t}{Z}. \quad (12)$$

In our case, with a Lagrangian given by (3), we can express it in a similar way, depending on link variables $J_{n,\mu}$, after making a change of variable $\Phi \rightarrow \sqrt{J} \xi$. Now, $J_{n,\mu} = \text{const} = J > 0$. This causes the appearance of a twist: the fields placed in the points $n, n+\mu$ connected by a link where $J_{n,\mu}$ has changed to $-J_{n,\mu}$ tend to change their signs: we have given rise to a topological excitation, with a nonzero topological charge $\Phi(x = \infty) - \Phi(x = -\infty)$.

We now define

$$C_\mu(t) = \langle \mu(n,t)\mu(n+\tau) \rangle, \quad (13)$$

where our path in the dual lattice will be the minimum length path connecting them, i.e., straight vertical lines.

The topological excitation (with nonzero projection on the soliton sector) appears at the time t , and annihilates at $t+\tau$. Thus, we expect an exponential behavior, similar to that of $C_\phi(t)$. In this case, one of the two paths connecting the points R_1 and R_2 has a much bigger contribution to C_μ : that which crosses the dislocation. In fact, we have observed a clear exponential decay, $\langle \mu_{(n,t)}\mu_{(n,t+\tau)} \rangle \sim \exp\{-C\tau\}$, and therefore we obtain the soliton mass as

$$m_{\text{sol}} = \ln \frac{C_\mu(t)}{C_\mu(t+1)}. \quad (14)$$

When we study $\langle \exp(-2 \sum_{n,\mu}^* \Phi_n \Phi_{n,\mu}) \rangle$, we must consider the risks of our method: we study a strongly nonlocal quantity, which is seriously affected by the finite size of our lattice. In addition, the use of an exponential function implies a magnification of errors.

In principle, we do not know to what point these effects will spoil our results. In order to control these risks, we look for an alternative way of calculating the soliton mass from local nonexponential variables. Following Groeneveld, Jurkiewicz, and Korthals Altes [8], we introduce a local parameter $\Omega(\beta)$, which accounts for the energy response to the appearance of the twist.

First, it will be useful to change the variables the action depends on. We note that, making the following change of variable, $\Phi \rightarrow \xi = \Phi/\sqrt{\beta_0}$ with $\beta=0=1/\lambda_0$, we obtain

$$\begin{aligned} Z(r_0, \lambda_0) &\equiv \hat{Z}(r_0, \beta_0) \\ &= \beta_0^{-V/2} \int_{-\infty}^{+\infty} (\prod_n d\xi_n) \exp \left\{ -\beta_0 \left[- \sum_{n,\mu} \xi_n \xi_{n,\mu} + \sum_n \left[\left(d + \frac{r_0}{2} \right) \xi_n^2 + \frac{1}{4!} \xi_n^4 \right] \right] \right\}, \end{aligned} \quad (15)$$

where $V=L^d$ is the volume of the system. The β_0 derivative of $Z(r_0, \lambda_0)$ is

$$\frac{\partial \hat{Z}(r_0, \beta_0)}{\partial \beta_0} = -\frac{V}{2} \frac{\hat{Z}(r_0, \beta_0)}{\beta_0} - \frac{1}{\beta_0} Z \langle S[r_0, \lambda_0] \rangle, \quad (16)$$

where $S(r_0, \lambda_0)$ is the action resulting from the integration of our Lagrangian (3).

If we impose antiperiodic boundary conditions in the spatial direction, we introduce a twist the length of which is the temporal dimension of the lattice, T . We can define the "twisted" partition function corresponding to this twist, $Z_t(r, \lambda) \equiv \hat{Z}_t(r, \beta)$. Keeping in mind (12) we can now calculate the soliton mass as

$$\begin{aligned} m_{\text{sol}} &= -\frac{1}{T} \ln \langle \mu(\mathbf{n}, T) \mu(\mathbf{n}, 0) \rangle \\ &= -\frac{1}{T} \ln \frac{Z_t(r_0, \lambda_0)}{Z(r_0, \lambda_0)} \\ &= -\frac{1}{T} \ln \frac{\hat{Z}_t(r_0, \beta_0)}{\hat{Z}(r_0, \beta_0)} = \int_{\beta_c}^{\beta_0} \Omega(\beta'_0), \end{aligned} \quad (17)$$

where β_c is the value for which our trajectory cuts the transition line between the $\langle \Phi^2 \rangle = 0$ and $\langle \Phi^2 \rangle \neq 0$ phases, and

$$\begin{aligned} \Omega(\beta_0) &= -\frac{1}{T} \frac{\partial}{\partial \beta_0} \ln \frac{\hat{Z}_t(r_0, \beta_0)}{\hat{Z}(r_0, \beta_0)} \\ &= \frac{1}{\beta_0} \frac{1}{T} \langle S_t(r_0, \lambda_0) \rangle_t - \langle S(r_0, \lambda_0) \rangle, \end{aligned} \quad (18)$$

where $\langle \rangle$ and $\langle \rangle_t$ stand for expectation values with Z (periodic boundary conditions) and Z_t (twisted or antiperiodic), respectively. We remark that in the Z_t system $\langle \Phi \rangle = 0$ in both the symmetric and broken phases. The integration in (17) implies defining a trajectory in the parameter space with r_0 fixed, and β starting from β_c . For higher values of β , we have no symmetry breaking, and the soliton mass vanishes. We will check the masses obtained with the exponential function by comparing them with those resulting from using Ω .

III. DETAILS OF THE SIMULATION

We have made use of a specially designed transputer-based parallel machine, RTN, including 64 T-805 processors distributed in 8 boards with 8 each. As an individual board calculates one point in the parameter space, we get eight absolutely independent groups of measurements for every (λ_0, r_0) . The error for every magnitude has been calculated averaging its eight independent predictions. We have used an adaptative Monte Carlo (MC) process so as to keep the rate of acceptance between 40 and 60 %.

We have simulated different lattice sizes ($16^2, 24^2, 48^2$) with (1000, 3000, 7000) iterations of thermalization and (2000, 22 500, 30 000) measurements. Within each transputer, we have taken (20, 10, 5) decorrelation MC iterations between two consecutive measurements. We have observed no relevant finite-size effects in the local quantities. However, big sizes are needed when computing

correlations, especially those defined by Kadanoff's operator, as a consequence of its strong nonlocality and its exponential form. As we have mentioned earlier, we cannot rely on the small-length correlations because of the contribution of large mass states; on the other hand, long-distance correlations are seriously affected by the finiteness of our lattice. Thus, in order to obtain a precise value for the mass from Kadanoff's operator we have needed bigger and bigger lattices.

IV. PHASE DIAGRAM AND THE SCALING REGION

Our model exhibits two phases. Classically, for positive values of r_0 the minimum energy configuration is $\Phi = 0$; for negative r_0 , a spontaneous symmetry breaking occurs, and the new minima are $\Phi = \pm \sqrt{6|r_0|}/\lambda_0$.

When we consider the contributions of all the configurations, each weighted with $\exp\{-S_{\text{Euc}}\}$, for small negative values of r_0 both minima are very close to each other and are not deep enough to stop fluctuations from restoring the symmetry. More negative values of r_0 are necessary to ensure that we are in the broken phase. Therefore, in the semiplane with negative r_0 there is a transition line separating both phases.

In order to determine the transition line, we choose several values of λ_0 . For each of them, we decrease r_0 until $\langle \Phi^2 \rangle$ becomes different from zero; in the limit of an infinite volume, its value passes from zero to a finite nonzero value when crossing the transition line; in a finite-volume system in the symmetric phase, $\langle \Phi^2 \rangle \approx 1/\sqrt{V}$, and what we see is a sharp rise of $\langle \Phi^2 \rangle$ (technically, in a finite lattice $\langle \Phi \rangle$ is not a good order parameter because tunneling between states with positive and negative values of the field cause it to be equal to zero all over the parameter space). Another useful quantity as an order parameter is the soliton mass. When computing $\langle \exp\{-2J \sum \Phi_n \Phi_{n+\mu}\} \rangle$, if we are in the $\langle \Phi^2 \rangle = 0$ phase, the values of Φ_n fluctuate around zero, and their sum over the path vanishes; the expected values appearing in (14) become independent of the length of the

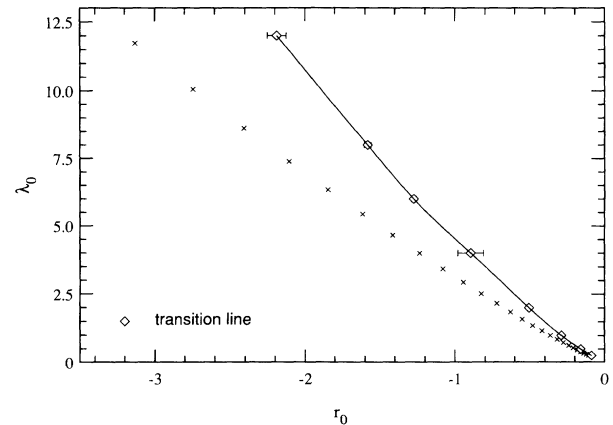


FIG. 1. The renormalization group trajectory followed starting from the initial values $r_0 = -0.105$, $\lambda_0 = 0.25$ is shown. The transition line between the $\langle \Phi^2 \rangle = 0$ and $\langle \Phi^2 \rangle \neq 0$ phases is drawn.

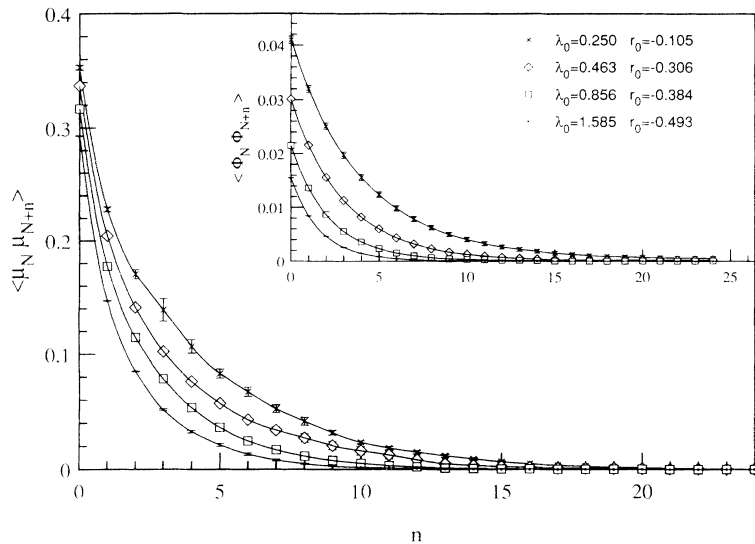


FIG. 2. Decay of the correlation functions $\langle \mu\mu \rangle$ and $\langle \Phi\Phi \rangle$ in a 48^2 lattice. While the latter decays quickly to 0, $\langle \mu\mu \rangle$ is noncompatible with 0 for large distances if we are near the Gaussian point. Thus, we expect the value of the mass we calculate from it to improve as we increase the lattice length.

path and equal to 1 and m_{sol} is zero. On the other hand, we expect nonzero m_{sol} for the symmetry broken phase, where the $\sum \Phi_n \Phi_{n+\mu}$ is different from 0. We determined the transition line using both parameters ($\langle \Phi^2 \rangle$ and m_{sol}). It is shown in Fig. 1.

In the region where $|r_0|/\lambda_0$ is large enough, we can compare them with mean-field predictions. Theoretically, $|\Phi| = \sqrt{6}|r_0|/\lambda_0$. In this region the fluctuations are small, and thus we have

$$\left\langle \exp \left[-2J \sum_L \Phi_n \Phi_{n+\mu} \right] \right\rangle \sim \exp \{ -2JL |\Phi^2| \},$$

where L is the length of the summation path, and we can consider $\langle \Phi(0)\Phi(r) \rangle \sim |\Phi^2|$ and therefore $m_{\text{sol}} = 2J|\Phi^2|$. Our results agree with these predictions.

Now we pass to determine the scaling region. We keep ourselves in the $\langle \Phi^2 \rangle \neq 0$ phase, where m_ρ and m_{sol} are different from zero. The reason for this is that, proceeding in this way, the continuum limit of our theory will correspond to the symmetry broken phase of the continu-

um problem, which is the one we are interested in. Thus, our next step is finding the region in the parameter space where Eqs. (6) are valid.

Along a RGT we expect to find constant values for the physical meaningful variables, such as the correlation length ξ , the physical masses M , etc. In the lattice we work with dimensionless quantities depending on the point of the trajectory $[\xi_0(r_0, \lambda_0), m(r_0, \lambda_0), \dots]$, related to the physical ones by $M = m/a$, $\xi = a\xi_0 \dots$. Consequently, although our lattice-defined quantities vary, the ratios m_ρ/m_{sol} , m_ρ^2/λ_0 , $m_{\text{sol}}^2/\lambda_0$, which are equal to the physical expressions M_ρ/M_{sol} , M_ρ^2/λ , M_{sol}^2/λ , remain constant along these trajectories.

We start from different points in the parameter space (r_0, λ_0) near to the critical point ($-0.2 < r_0 < 0$, $\lambda_0 = \text{fixed} = 0.1$). Iterating renormalization group transformations [Eq. (6), where we choose $s = 1.08$], we get further and further away from the origin (and thus from the continuum limit), drawing a series of trajectories. Along each one of them, we calculate the previously defined ratios in the different points obtained by the

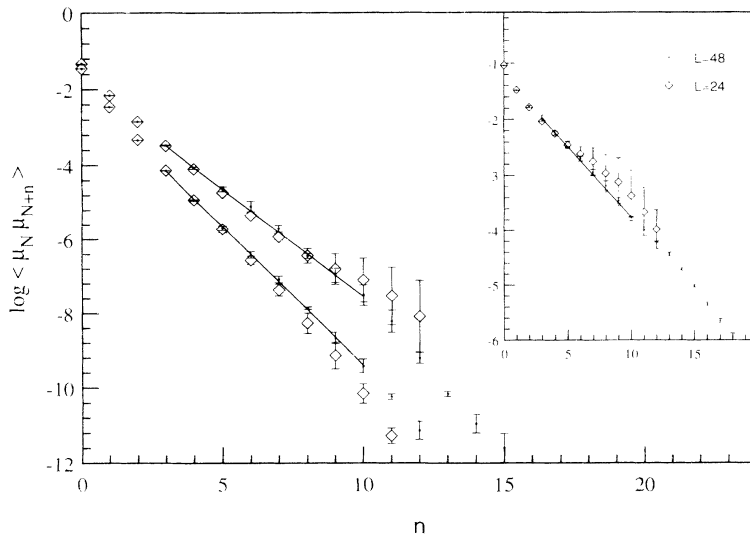


FIG. 3. Logarithm of the correlation function $\langle \mu\mu \rangle$ for three different points in the parameter space: for the small window at right, $\lambda_0 = 0.25$, $r_0 = -0.105$. The two other points are $\lambda_0 = 2.934$, $r_0 = -0.945$ and $\lambda_0 = 5.431$, $r_0 = -1.616$. Both are inside the scaling region. The latter is the one with the largest slope (the biggest mass).

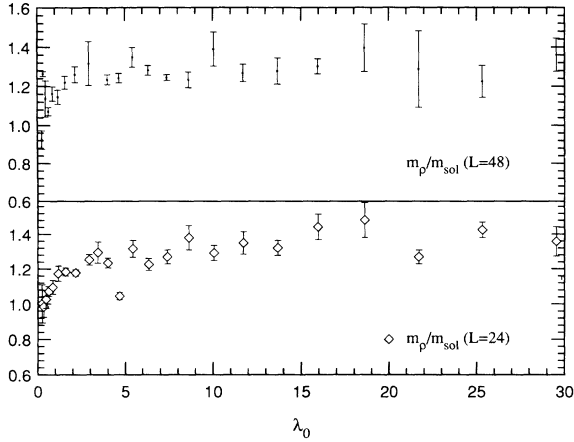


FIG. 4. Evolution of the ratio m_ρ/m_{sol} along the RGT previously drawn in Fig. 1. From the results in the 48^2 lattice, we see that the ratio becomes constant from $\lambda_0 \sim 1.5$, a fact which is not apparent in the 24^2 lattice. This gives us a lower limit for the section of our RGT inside the scaling region.

transformations. For every trajectory, we find a segment where these quantities remain approximately constant; the union of all the segments gives us the scaling region.

Initially, we follow curves near the transition line separating the $\langle \Phi^2 \rangle = 0$ and $\langle \Phi^2 \rangle \neq 0$ phases. As we move away from it, we find that the length of the segment reduces. This is clear because we need a large lattice correlation length in order to reproduce the continuum limit, and the region close to the line transition is appropriate to that. Far from this line the correlation length is small, and the discretization is important.

Finally, we choose a curve near that line, with the initial values ($r_0 = -0.105$, $\lambda_0 = 0.25$) (see Fig. 1). At this point we can illustrate our comments about the difficulties derived from the use of Kadanoff's operator. In Fig. 2 we represent the correlations of the fields Φ and μ for some points of this trajectory. As expected, when we get near the Gaussian point, the correlation length in-

creases, the mass is lower and the correlation decreases more and more slowly. For small enough values of the parameters, the correlation function $\langle \mu_N \mu_{N+n} \rangle$, for distances of the order of the length of the lattice, is not compatible with zero. (n is the distance in units of the lattice spacing.) Thus, we must be very careful when we calculate masses in this region.

There is another reason that makes it desirable to work with big lattices. Our method for calculating the masses consists basically of finding a certain correlation function, and fitting it to an exponential, or to a hyperbolic cosine. We expect this fit to be reasonably good for a set of intermediate values of n . When n approaches the length of the lattice—in our case, half this length, because of the periodic boundary conditions—the fit is not possible any longer. The bigger our lattice is, the longer this well-fitting segment becomes, and we have more points to fit our theoretically predicted behavior, and so calculate the mass with higher precision. This is clearly shown in Fig. 3: in the plot at left we draw the logarithm of the correlation function $\langle \mu_N \mu_{N+n} \rangle$ for 24^2 and 48^2 lattices, in a region far from the Gaussian point. In the small lattice, when $n \sim 9$, the fitting to a straight line is no longer possible, while in the big one we can still include some more points and get a good fit to a straight line. In the small picture at right, the parameters are $\lambda_0 = 0.25$, $r_0 = -0.105$; we have seen in Fig. 2 that, for these values, the correlation length is comparable with the lattice length, and we expect serious corrections. In fact, for the small lattice, the agreement region is smaller.

In Fig. 2 we see that the function $\langle \Phi_N \Phi_{N+n} \rangle$ is much smaller than the μ correlation, and we expect that the values obtained for the boson mass are not so strongly affected by the size of the lattice. Our results confirm this prediction.

Now we can estimate the scaling region. From Fig. 4, we see that it begins at $\lambda_0 \sim 2$, the value from which m_ρ/m_{sol} can be considered as a constant. The upper boundary of this region can be more clearly inferred from Fig. 5. We expect $m/\sqrt{\lambda_0}$ to be constant or, equivalent-

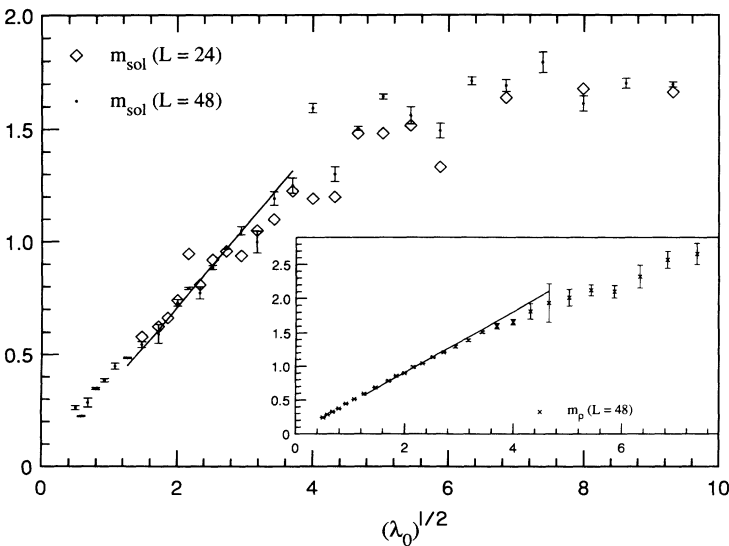


FIG. 5. m_ρ and m_{sol} vs $\sqrt{\lambda_0}$ along the RGT, for 24^2 and 48^2 lattices. We determine the scaling region by selecting the points which give a reasonable fit to a function $y = ax$. In this way, we find the upper limit of this region, given by $\lambda_0 \sim 14$. For m_ρ only the results from the 48^2 lattice are drawn because they coincide with those from the small lattice.

ly, a linear behavior of m with $\sqrt{\lambda_0}$, m tending to zero as $\sqrt{\lambda_0}$ does. Thus, for the RGT starting from the initial values $\lambda_0=0.25$, $r_0=-1.05$, the scaling region corresponds to the interval $1.5 < \lambda_0 < 14$.

V. RESULTS

A. Results from the operators

First of all, we want to check that what we call soliton mass, calculated using Kadanoff's operator, really behaves as a mass. We will compare its evolution under the renormalization group equations to that of the fundamental boson mass. On the other hand, we compare its value to previous theoretical predictions.

A quantity Θ_{phys} with dimension $[\Theta]$ is related to its equivalent in the lattice Θ_{latt} by $\Theta_{\text{phys}} \sim a^{[\Theta]} \Theta_{\text{latt}}$. As we are working in less than four dimensions, we can keep λ fixed, and $\lambda_0 \sim \lambda a^2$ tends to 0 as a^2 when we approach the continuum limit (Gaussian fixed point) along a RGT. We also expect finite values for M_ρ , M_{sol} , so our value of the masses in the lattice $m \sim Ma$ tends to 0 as a .

From that we deduce, as we approach the continuum limit, $m_{\text{sol}} \sim \sqrt{\lambda_0}$. Figure 5 shows that, within the limit of the scaling region, that is the behavior of m_ρ and m_{sol} .

In a system with only one relevant direction, the renormalized trajectory coincides with that direction. In our case we have a twice-unstable point, and there is a continuous family of renormalized trajectories leaving it, each of them corresponding to a different continuum theory. In the previous section we have chosen one of those trajectories; once we give an arbitrary value of λ , M_ρ , and M_{sol} can be calculated as $M = (m/\sqrt{\lambda_0})\sqrt{\lambda}$. In our RGT, $M_\rho = 0.453\sqrt{\lambda}$ and $M_{\text{sol}} = 0.356\sqrt{\lambda}$. Next we study the evolution of M_{sol} when, starting from a point on the transition line, we move further and further into the symmetry broken phase. First, let us summarize some qualitative basic ideas. When we quantize the classical absolute minimum, we obtain the vacuum of the quantum theory; quantization around the soliton gives us the soliton sector. If this local minimum is broad (which, in our case, corresponds to a point near the transition line between $\langle \Phi^2 \rangle \neq 0$ and $\langle \Phi^2 \rangle = 0$), a great number of configurations different from the classical solution will contribute to the value of any observable. But as we move away from this zone, the potential well gets deeper and deeper, and a moment comes when we have contributions only from the minimum and configurations very close to it; we are recovering the classical solution.

In order to explore these ideas, we trace a trajectory in (λ_0, r_0) space fixing $r_0 = -2.2$ and letting λ_0 move from the vicinity of the transition line ($\lambda_0 \simeq 12$) deeper and deeper into the $\langle \Phi^2 \rangle \neq 0$ phase. This path cuts a different RGT in each of its points (with different physical masses for a value of λ).

To calculate the classical continuous limit for the soliton mass, we make use of the fact that, in a continuous Euclidean space, a soliton of the $\lambda\Phi^4$ classical theory in $1+1$ dimensions propagating with a velocity v is given by [7]

$$\Phi(x, t) = \left[\frac{6|r|}{\lambda} \right]^{1/2} \tanh \left[\frac{|r|^{1/2}}{\sqrt{2}} \left[\frac{x-vt}{\sqrt{(1-v^2)}} \right] \right]. \quad (19)$$

The energy density is $\epsilon(x)$, the expression of which coincides with the Euclidean Lagrangian. The classical absolute minimum is $\Phi = \pm\sqrt{6|r|/\lambda}$. At a classical level, we can define the soliton mass as

$$M_{\text{class}} = E - E_{\text{min}} = 4\sqrt{2} \frac{|r|^{3/2}}{\lambda}, \quad (20)$$

E_{min} being the energy of the absolute minimum, and E that of the soliton solution.

When we quantize the soliton, in the weak-coupling approximation ($\hbar\lambda/r \ll 1$), the mass obtained is, up to an order $\mathcal{O}(\hbar\lambda/|r|)$ [7],

$$M_{\text{quantum}} = M_{\text{class}} + \hbar\sqrt{r} \left[\frac{1}{6}\sqrt{3/2} - \frac{3}{\pi}\sqrt{2} \right]. \quad (21)$$

We have taken all along \hbar equal to 1.

Comparing our results for m_{sol} to those predicted by expression (21) (see, e.g., Fig. 7), we see a clear linear behavior with $\beta_0 = 1/\lambda_0$. That behavior is intermediate between the order 0 and $\mathcal{O}(\hbar)$ theoretical predictions, closer to this second one. That displacement with respect to the $\mathcal{O}(\hbar)$ predictions may be attributed to the contribution of higher orders in $\hbar\lambda_0/|r_0|$.

B. Results from twisted system

The use of twists is known to be, in a computer-simulated theory, a good help for studying the phase structure. Our main motivation for introducing it is to calculate m_{sol} in an alternative way to the use of Kadanoff's operator, so avoiding its risks, already mentioned in Sec. II.

We impose antiperiodic boundary conditions in the spatial coordinate. In this way, we introduce a twist in the lattice that lasts from $t=0$ to T . We evaluate the expected value of the action under these conditions, $\langle S_t \rangle_t$, following the notation introduced in Sec. II. In the $\langle \Phi^2 \rangle = 0$ phase, because of its $\pm\Phi$ symmetry, changing the signs of some \mathcal{J} 's does not cause the expected value of the action to change, and $\langle S \rangle = \langle S_t \rangle_t$. That means $M_{\text{sol}} = 0$, or we can also see the vacuum as a "soliton condensate." However, in the $\langle \Phi^2 \rangle \neq 0$ phase things are not so any longer. By inducing the twist, we favor the appearance of a soliton propagating through time. $\delta S = \langle S_t \rangle_t - \langle S \rangle$ is the energetic response of the lattice to the introduction of the twist; it must be related to the Euclidean energy of the soliton, as we will see.

As we did in the previous section, we follow the path fixing the value of $r_0 = -2.2$. δS must increase its value from 0 near the transition line to the classically predicted one. Again, we plot δS against $|r_0|^3/\lambda_0^2$. In Fig. 6, we can see that it grows up steeply and soon stabilizes at the classical value (20): $|\delta S|^2/\lambda_0 = 32|r_0|^3/\lambda_0^3$. Instead of λ_0 we have drawn $\beta_0 = 1/\lambda_0$.

Intuitively, there is a relationship between δS and the soliton mass, which is its minimum energy level. In the

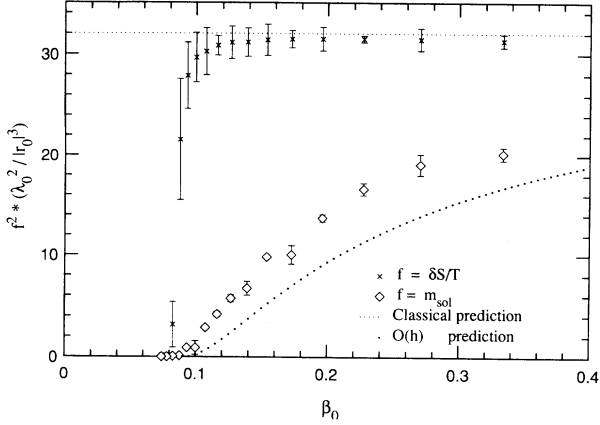


FIG. 6. In a 48×48 lattice, along the $r_0 = -2.2$ vertical path, the evolution of the quantities $(\delta S/T)(\lambda_0^2/|r_0|^3)$ and $m_{\text{sol}}^2(\lambda_0^2/|r_0|^3)$ vs $\beta_0 = 1/\lambda_0$ is shown. The classical value for both ratios is 32. The results are compared to those for the perturbative calculation up to an order $O(\lambda_0/|r_0|)$. While all these results coincide in the limit $(\lambda_0/|r_0|) \rightarrow 0$, $(\delta S/T)$ soon stabilizes at the classical value, while m_{sol} keeps closer to the first-order calculation.

classical limit, $\delta S/T$ is equal to m_{sol} . In Fig. 6, we see that, as we increase β_0 , both values tend to coincide. In general, the expression relating both quantities can be obtained if we keep in mind (17) and (18):

$$m_{\text{sol}} = \frac{1}{T} \int_{\beta_c}^{\beta} \frac{\delta S(\beta')}{\beta'} . \quad (22)$$

From Fig. 6, we see that $\delta S/T$ suffers a sharp increase around $\beta_0 = 0.0826$ ($\lambda_0 = 12.1$), indicating that we have crossed the transition line. We deduce $\beta_c = 0.0804 \pm 0.0022$, $\lambda_c = 12.45 \pm 0.35$. In order to avoid errors coming from the estimate of β_c and δS in the vicinity of that line, we take, instead of (22),

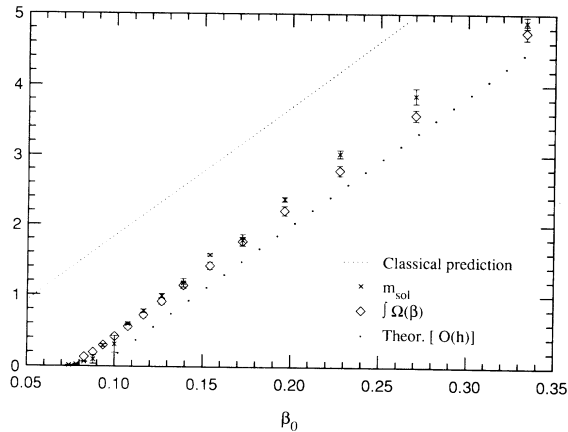


FIG. 7. For the 48×48 lattice, along the vertical path with $r_0 = -2.2$, the results for m_{sol} obtained from Kadanoff's operator and the mass given after the integration of $\Omega(\beta_0)$ are compared. We compare them with the classical and the theoretical perturbative value up to first order in $O(\lambda_0/|r_0|)$. The x coordinate is $\beta_0 = 1/\lambda_0$.

$$m_{\text{sol}}(\beta) = m_{\text{sol}}(\beta_i) + \frac{1}{T} \int_{\beta_i}^{\beta} \frac{\delta S(\beta')}{\beta'} . \quad (23)$$

where we have taken $\beta_i = 0.0826$, the first value of β for which δS is clearly nonzero. We fit our values of m_{sol} to a straight line, and take $m_{\text{sol}}(\beta_i)$ to be the height of the line at β_i .

We compare the results obtained applying (17) with those from Kadanoff's operator (see Fig. 7). Both values coincide with a precision up to 3 in the least favorable point.

VI. CONCLUSIONS

We have studied topological excitations in the $(\lambda\phi^4)_{1+1}$ model on the lattice using a “disorder parameter,” from the decay of which we can compute the soliton mass. The results obtained have a well-defined continuum limit, which we have computed with the renormalization group equations. We have paid special attention to make sure that we are working in the scaling region, where physical quantities are unchanged along the RGT. We have also computed the soliton mass from the difference of the vacuum energy between the twisted and untwisted systems, where quantities are local, and we found this result agrees with the previous one.

Now we would like to compare both methods: the first has the disadvantage that it implies the calculus of operators which are strongly nonlocal and exponential, and thus the method is very sensitive to finite-size effects and systematic errors. A lot of statistics is necessary to obtain results within a reasonable margin of error. On the other hand, the method using twisted systems decreases considerably the computation time required. The statistic errors are small, and thus we conclude that imposing twisted conditions is a very satisfactory alternative in order to calculate the soliton mass. However, twisted conditions modify the vacuum of the theory, and make the calculation of other masses to which to compare the results (such as, e.g., the fundamental boson mass) impossible.

We have compared our nonperturbative result for the mass of the topological excitations in the continuum limit with the theoretical perturbative result up to first order. Our results show a systematic lineal raise, which may be due to higher-order corrections not considered in the perturbative prediction.

The inclusion of fermions with a Yukawa coupling to the scalar fields is a very interesting future work. In this case we have a three-parameter space and a very rich model. The problem is simplified by the fact that bosonization is possible, and so Monte Carlo simulation is simpler than when fermions are considered directly. Therefore, it must be also possible to compute the soliton mass and the continuum limit.

ACKNOWLEDGMENTS

We want to thank A. Cruz, L. A. Fernández, P. Di Giudice, and A. Grillo for their kind suggestions, and the RTN group for the use of the RTN machine.

- [1] G. Schierolz, J. Seixas, and M. Teper, *Phys. Lett.* **151B**, 69 (1985).
- [2] H. G. Evertz *et al.*, *Phys. Lett. B* **175**, 335 (1986); T. A. De Grand and D. Toussaint, *Phys. Rev. D* **22**, 2478 (1980).
- [3] V. Azcoiti, A. Cruz, G. Di Carlo, A. F. Grillo, and A. Tarancón, *Europhys. Lett.* **9**, 23 (1989).
- [4] K. G. Wilson and J. Kogut, *Phys. Rep.* **12**, 75 (1974); K. G. Wilson, *Rev. Mod. Phys.* **47**, 773 (1975).
- [5] L. P. Kadanoff, *Phys. Rev. Lett.* **23**, 1430 (1969); L. P. Kadanoff and H. Ceva, *Phys. Rev. B* **3**, 3918 (1971).
- [6] G. Fox, J. Gupta, O. Martin, and S. Otto, *Nucl. Phys.* **B205**, 188 (1982).
- [7] R. Rajaraman, *Solitons and Instantons* (North-Holland, Amsterdam, 1982).
- [8] J. Groeneveld, J. Jurkiewicz, and C. P. Korthals Altes, *Phys. Scr.* **23**, 1022 (1981).